DOI: 10.1007/s11099-017-0701-8 PHOTOSYNTHETICA 56 (2): 633-640, 2018

Simulation of PSII-operating efficiency from chlorophyll fluorescence in response to light and temperature in chrysanthemum (*Dendranthema grandiflora*) using a multilayer leaf model

E. JANKA[*,+], O. KÖRNER[**], E. ROSENQVIST[***], and C.-O. OTTOSEN[****]

Department of Process, Energy and Environmental Technology, University College of Southeast Norway, Kjølnes Ring 56, 3918 Porsgrunn, Norway[*]
Department of Plant Technology, AgroTech, Danish Technological Institute, Højbakkegård Allé 21, DK-2630 Taastrup, Denmark[**]
Department of Plant and Environmental Sciences, Crop Science, University of Copenhagen, Højbakkegård Allé 9, DK-2630 Taastrup, Denmark[***]
Department of Food Science – Plant, Food and Climate, Aarhus University, Kirstinebjergvej 10, DK-5792 Årslev, Denmark[****]

Abstract

Chlorophyll fluorescence serves as a proxy photosynthesis measure under different climatic conditions. The objective of the study was to predict PSII quantum yield using greenhouse microclimate data to monitor plant conditions under various climates. Multilayer leaf model was applied to model fluorescence emission from actinic light-adapted (F') leaves, maximum fluorescence from light-adapted (F_m') leaves, PSII-operating efficiency (F_q'/F_m'), and electron transport rate (ETR). A linear function was used to approximate F' from several measurements under constant and variable light conditions. Model performance was evaluated by comparing the differences between the root mean square error (RMSE) and mean square error (MSE) of observed and predicted values. The model exhibited predictive success for F_q'/F_m' and ETR under different temperature and light conditions with lower RMSE and MSE. However, prediction of F' and F_m' was poor due to a weak relationship under constant ($R^2 = 0.48$) and variable ($R^2 = 0.35$) light.

Additional key words: extreme climate; greenhouse; monitor; paradermal layer; photosynthesis.

Introduction

Chlorophyll (Chl) fluorescence is a sensitive and relatively simple noninvasive approach applied under a range of controlled and field conditions to monitor plant photosynthetic performance (Baker and Rosenqvist 2004, Baker 2008, Murchie and Lawson 2013, Guo and Tan 2015). The PSII-operating quantum efficiency in leaves is linearly related to CO_2 assimilation (Genty *et al*. 1989, Harbinson *et al*. 1990), which resulted in wider applications of Chl fluorescence as a plant monitoring tool (Baker and Rosenqvist 2004, Baker 2008, Murchie and Lawson 2013, Guo and Tan 2015). Photosynthetic rate is the product of absorbed irradiance and quantum yield, and quantum yield depends on absorbed irradiance and photosynthetic capacity (Evans 1995).

Vogelmann and Han (2000) resolved light absorption and carbon fixation profiles in leaves using Chl imaging to measure Chl fluorescence profiles in spinach, which is used as a valid measure of light absorption and carbon fixation (Evans and Vogelmann 2003). A measured Chl fluorescence profile was applied, and the light absorption and CO_2 fixation under a range of conditions was successfully estimated and tested against the prediction using a multilayer leaf model. The model was congruent with the gas-exchange data, and was largely consistent

Received 23 September 2016, *accepted* 2 December 2016, *published as online-first* 9 February 2017.
[+]Corresponding author; phone: +4741509113, e-mail: eshetu.j.wakjera@usn.no.
Abbreviations: Chl – chlorophyll; ETR – electron transport rate; F' – fluorescence emission from actinic light; F_m' – maximum fluorescence from light-adapted leaves; LED – light emitting diode; PAM – pulse amplitude modulated; NPQ – nonphotochemical quenching; F_q'/F_m' – PSII-operating efficiency; MSE – mean square error; RMSE – the root mean square error.
Acknowledgements: This research was part of the project itGrows, and as such, the authors would like to thank co-funding provided by the Danish High Technology Foundation. Additional funding was provided by the European Regional Development Fund Grant No. 35-2-10-11 (ERDF) and EU project GreenGrowing.

with conventional Chl fluorescence data (Vogelmann and Evans 2002, Evans and Vogelmann 2003, Evans 2009).

Evans (2009) applied the multilayer leaf model, and revealed potential errors in calculating electron transport rates from Chl fluorescence measurements. Therefore, the model was revised and a new approximation of PSII quantum yield was calculated, and used to generate maximum fluorescence from light-adapted leaves (F_m'), and fluorescence emission from actinic light-adapted leaves (F'). The revised model assumes F' is constant and proportional to the light absorbed, which was validated by measurement from several plant species (Evans 2009).

Chrysanthemum is an ornamental crop widely grown for cut flowers and as pot plants (Van der Ploeg and Heuvelink 2006). Chl fluorescence as a noninvasive approach has been used to monitor and detect high temperature stress in chrysanthemum (Janka *et al*. 2013, Janka *et al*. 2015). However, as such, online measurements of Chl fluorescence combined with model prediction are not yet frequently used to monitor plant conditions under extreme microclimates.

The new approximation of PSII quantum yield is simple and straightforward to simulate under different light and temperature conditions. In our simulation model, we used a linear function for estimating F' from measured data, and electron transport as a function of irradiance with the temperature function of maximum electron transport (Farquhar *et al*. 1980, Yin and Struik 2009) implemented within the multilayer leaf model. Our primary objective was to compare the model simulation with the actual measurements derived from Chl fluorescence parameters. Congruence between model simulation and empirical data can contribute substantially to our progress in combining model prediction and online measurement of Chl fluorescence parameters to monitor plant conditions under different microclimatic conditions.

Materials and methods

Plant material: Chrysanthemum (*Dendranthema grandiflora*) 'Coral Charm' cuttings were rooted in plastic pots (9.7 cm high and 11 cm in diameter) filled with a commercial peat mixed with granulated clay (*Pindstrup 2, Pindstrup A/S*, Ryomgaard, Denmark) at Aarhus University (Aarslev, Denmark 55°22' N). Plants were grown in a growth chamber (*MB-teknik*, Brøndby, Denmark) during spring/summer (6 April 2012 to 16 June 2012), and in a greenhouse during summer/fall (10 August 2012 to 10 September 2012), and used for continuous fluorescence measurements for calibration and validation of the model.

Plants were grown in the growth chamber under five temperature regimes (20, 24, 28, 32, 36°C), and four constant irradiance levels [117, 311, 485, 667 μmol (photon) m^{-2} s^{-1} PAR]. Plants were grown at a density of 40 plants m^2, and the air temperature set-point was 20/20°C. Supplemental nutrition (macronutrients: N 185 ppm, P 27 ppm, K 171 ppm, and Mg 20 ppm; micronutrients: Ca, Na, Cl 18 ppm, SO_4 27 ppm, Fe 0.9 ppm, Mn 1.17 ppm, B 0.25 ppm, Cu 0.1ppm, Zn 0.77 ppm, and Mo 0.05 ppm) was provided mixed with irrigation water, and automatically supplied twice a day as ebb-and-flood irrigation (08:45 and 16:15 h). Irrigation water electrical conductivity (EC) and pH were 1.88 μS cm^{-1} and 5.8, respectively. Biological controls against insects were used twice during the growing period.

Chl fluorescence was measured continuously for three days in the growth chamber, and five consecutive days in the greenhouse using monitoring-*PAM* or multi-channel Chl fluorometer (*Walz, Eifeltrich*, Germany) with four measuring heads (*Moni-head/485*). The *Moni-PAM* heads were connected using the Moni-bus (*Field bus, RS485*) to a computer controlled by software (*WinControl–3*, *version 2.xx*). The Moni-PAM measured fluorescence of actinic light-adapted leaves (F'), maximum fluorescence from light-adapted (F_m') leaves, PSII operating efficiency (F_q'/F_m'), electron transport rate (ETR), PAR, and leaf temperature. The saturating pulse for fluorescence measurements was recorded every 30 min to avoid potential photoinhibition. The measuring and actinic light was blue power LED (peak wavelength: 450 nm, full width at half maximum is 18 nm). The intensity of the measuring light was 0.1 to 1 μmol(photon) m^{-2} s^{-1} at F_0 and F_t and 1 to 15 μmol(photon) m^{-2} s^{-1} at F_m. The intensity of the maximum photosynthetically active radiation of actinic light and saturating pulse were 1,500 and 3,500 μmol (photon) m^{-2} s^{-1}, respectively.

Models: The multilayer model (Evans and Vogelmann 2003, Evans 2009) was used to model PSII-operating quantum efficiency. The multilayer model is based on paradermal leaf sections (leaf cross-sections), and for each section the fraction of light absorbed is defined as:

$$I_1 = I\ \alpha\ \beta\ a_1 \quad (1)$$

where I is incident irradiance, α is leaf absorbance, β is the fraction of light absorbed by PSII, and a_1 is the fraction of light absorbed in layer one. However, the model assumes uniform light intensity and constant biochemical composition through a given leaf (Farquhar *et al*. 1980), consequently the model considers a single paradermal leaf layer. The electron transport rate for layer one is calculated as a nonrectangular hyperbolic function of irradiance (Evans 2009, Yin and Struik 2009). In the model, θ is assumed to be 0.85. The modelled rate of electron transport for the entire leaf is calculated as follows:

$$J_1 = \left\{I_1 + J_{max,1} - \left[\left(I_j + J_{max,1}\right)^2 - 4\,\theta\ I_1\ J_{max,1}\right]^{0.5}\right\}/(2\ \theta) \quad (2)$$

Maximum electron transport ($J_{max,1}$) temperature dependency is calculated using the biochemical model temperature function for C_3 photosynthesis (Farquhar *et al*. 1980), and following Gijzen (1995):

$$J_{max,1} = J_{max,25}\ e^{\left(E_J \frac{T_l - T_{25}}{T_l . R . T_{25}}\right)} . \left[1 + e^{\frac{(S-H)/T_l}{R}}\right] . \left[1 + e^{\frac{(S-H)/T_{25}}{R}}\right]^{-1} \quad (3)$$

Therefore, the quantum yield of layer one is calculated as:

$$F_{q'}/F_{m',1} = J_1/I_1 \quad (4)$$

The PSII operating efficiency of a leaf is derived from the fluorescence of actinic light-adapted (F') leaves, and maximum fluorescence from light-adapted (F_m') leaves, using the following equation (Genty *et al*. 1989, Baker and Rosenqvist 2004):

$$F_{q'}/F_{m'} = 1 - F'/F_{m'} \quad (5)$$

Evans (2009) used a new approximation method to calculate fluorescence of an actinic light adapted leaf (F'), where a relationship is developed between F' and the light absorbed by PSII. In the model, the linear relationship between F' and irradiance was provided as follows:

$$F'_{,1} = I_1\ c + k \quad (6)$$

where c is the slope and k is the intercept, which were estimated from the linear relationship between irradiance absorbed by PSII and measured F'. The calculated F' is used with the following equation to derive F_m':

$$F_{m',1} = I_1\ c + k/\left(1 - F_{q'}/F_{m',1}\right) \quad (7)$$

The total calculated quantum yield for the leaf is the sum of F' and F_m' for each layer, and the PSII operating efficiency is derived as follows:

$$\frac{F_{q'}}{F_{m',1}} = 1 - \frac{\Sigma(I_1\ c+k)}{\Sigma\left(I_1/(1 - F_{q'}/F_{m',1})\right)} \quad (8)$$

Following Genty *et al*. (1989), the leaf ETR is calculated from the *fluorescence* measurement:

$$ETR = F_{q'}/F_{m'}\ I\ \alpha\ \beta \quad (9)$$

The calculated ETR from the calculated leaf quantum yield is calculated as:

$$ETR_{,1} = F_{m'}/F_{m',1}\ I\ \alpha\ \beta \quad (10)$$

Statistical analysis: The multilayer leaf model was written in computer programming language for mathematical computing and simulation, *MATLAB* (*version 7.11.0, MathWorks, Natick*, MA, USA). The nonlinear (weighted) least-squares estimates of the model parameters were completed in the programming language *R* (*R version 2.15.0*, www.r-project.org). Model performance was evaluated by linear regression to test the model prediction against the observed values (Retta *et al*. 1991). *SigmaPlot 11.0* (*Systa software, Inc*., Washington, USA) was employed to generate graphics. Model performance was evaluated by comparing the differences between the root mean square error (RMSE) and mean square error (MSE) of observed and predicted values.

Results

Regression analyses were performed between several fluorescence measurements, including actinic light-adapted leaves (F') and maximal fluorescence (F_m'), and light-adapted leaves under constant (*i.e.* growth chamber) and variable (*i.e.* greenhouse) light conditions. A weak and positive relationship between F' and irradiance in both uniform and variable irradiance conditions were detected (R^2 = 0.48 and 0.35, respectively) (Fig. 1*A,C*). The slope of the linear relationship showed the rate of increase in F' with increased irradiance was higher under variable than that under uniform irradiance conditions. The F_m' decreased under increased irradiance in both uniform and variable light conditions (Fig. 1*B,D*). However, the decrease in F_m' was more rapid under constant irradiance than that of variable irradiance conditions.

F_q'/F_m', ETR, F', and F_m' were predicted at different temperatures using the model and compared to measured data. The model successfully predicted F_q'/F_m' and ETR (Fig. 2*A,B*) at 24°C with lower RMSE between predicted and observed. However, the model was moderately successful in predicting F' and F_m' with a relatively high residual MSE between predicted and observed values (Fig. 2*C,D,* Table 1). The model was successful in predicting ETR at 24°C and F_q'/F_m' at 28°C (Fig. 3*A*,*B*; Table 1). At 28°C, the model showed increased accuracy in predicting F_m' than that at 24°C, with lower RMSE (Fig. 3*C,D*), even though the model relatively predicted well F' at 24°C.

The model behaviour was investigated by simulating three different temperature regimes (Fig. 4). The simulation showed F_q'/F_m', ETR, and F_m' differed at different temperatures, but not F′. F_q'/F_m' decreased with increased light and ranged between 0.72–0.18. The minimum value was predicted for 20°C with an irradiance of 1,500 μmol(photon) m^{-2} s^{-1} (Fig. 4*A*). The model simulated the highest ETRs for 28°C and the lowest for 20°C. F' increased with light from a minimum of 410 to a maximum of 668; no change was observed with temperature. However, F_m' showed temperature differences, ranging from 1,398 at the lowest irradiance for all temperatures, and 794 at the highest irradiance for 20°C (Fig. 4*D*). In the simulation, F_m' showed the greatest differences between temperatures within the light range of 200–800 μmol(photon) m^{-2} s^{-1}.

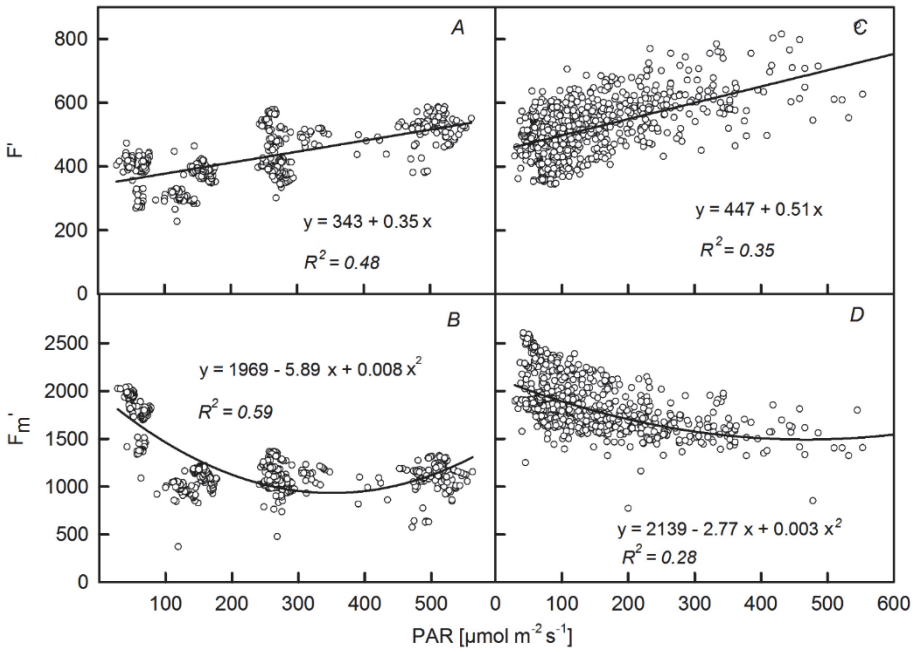

Fig. 1. The fluorescence emission from a leaf adapted to actinic light (F') measured in a growth chamber (*A*) and in a greenhouse (*B*), and maximal fluorescence (F_m') from a light-adapted leaf in a growth chamber (*C*) and in a greenhouse (*D*) as a function of light. The growth temperature was 20°C in the growth chamber and 22°C (± 1.31) in the greenhouse, CO_2 was 600 µmol mol^{-1}. The fluorescence was measured continuously every 30 min using a monitoring PAM. A linear function was fitted to the relationship between F' and PAR and a second order polynomial function was fitted to the relationship between F_m' and PAR.

Table 1. Evaluation of the model performance of the observed and predicted values of each variable using the mean bias error (MBE) and the root mean square error (RMSE) at five temperatures. MBE is a sum of the difference between simulated and measured divided by the number of observations, whereas RMSE is a square root of the sum of squared diffference between the simulated and measured divided by the number of observations.

Parameter	Temperature [°C]									
	20		24		28		32		36	
	MBE	RMSE	MBE	RMSE	MBE	RMSE	MBE	RMSE	MBE	RMSE
F'	36.03	71.21	–8.28	66.98	19.57	67.85	–58.12	108.96	–83.52	124.56
F'_m	–79.59	358.06	–50.87	236.05	–44.86	219.46	–88.44	551.74	–171.39	396.36
F'_q/F'_m	–0.04	0.06	0.00	0.06	–0.03	0.05	0.07	0.11	0.04	0.05
ETR	–3.83	7.65	–0.43	6.25	–1.82	6.73	12.01	18.29	6.07	9.37

F_q'/F_m', ETR, F', and F_m' simulations were performed using irradiance and temperature as input variables over the course of each day (Figs. 5, 6). The F_q'/F_m' model simulations were accurate relative to data observations throughout the day on day three of the observations (Fig. 5*A*), and fair throughout the day on day six of the observations (Fig. 6*A*), however, simulations predicted actual observations less well for early morning and late afternoons on those days. ETR was successfully simulated for both observation days following the daily course of variation in light. However, the model simulated F' and F_m' with less accuracy on both treatment days (Figs. 5*C*,*D*; 6*C,D*). The simulated F' was nearly constant on observation of the day three (Fig. 5*C*), with little variation over the course of the day, while actual measurements of F' showed more variation during the day. Similarly, simulated F_m' was not congruent with observations on observation of the day three, and notable variation between simulated and observational data was found for the early morning and late afternoon (Fig. 5*D*). F' and F_m' model simulations were more accurate compared to measurement data on treatment of the day six, particularly near midday (Fig. 6*C,D*), however, greater variation between simulated and measured data was observed in the early morning and late the afternoon for both fluorescence parameters.

Discussion

The positive linear increase in F' (Fig. 1*A,C*) and decrease in F_m' (Fig. 1*B,D*), with increased irradiance is a common fluorescence trend associated with PSII reaction centres. Maxwell and Johnson (2000) observed an increase in Chl fluorescence yield during the first illumination similar to F', however, the F_m' generated by the saturating-irradiance pulse decreased with increased irradiance due to fluorescence quenching, also known as nonphotochemical quenching processes (NPQ) (Maxwell and Johnson 2000, Baker and Rosenqvist 2004). In the present study, greenhouse irradiance levels were more variable compared to the uniform irradiance conditions in the growth chamber

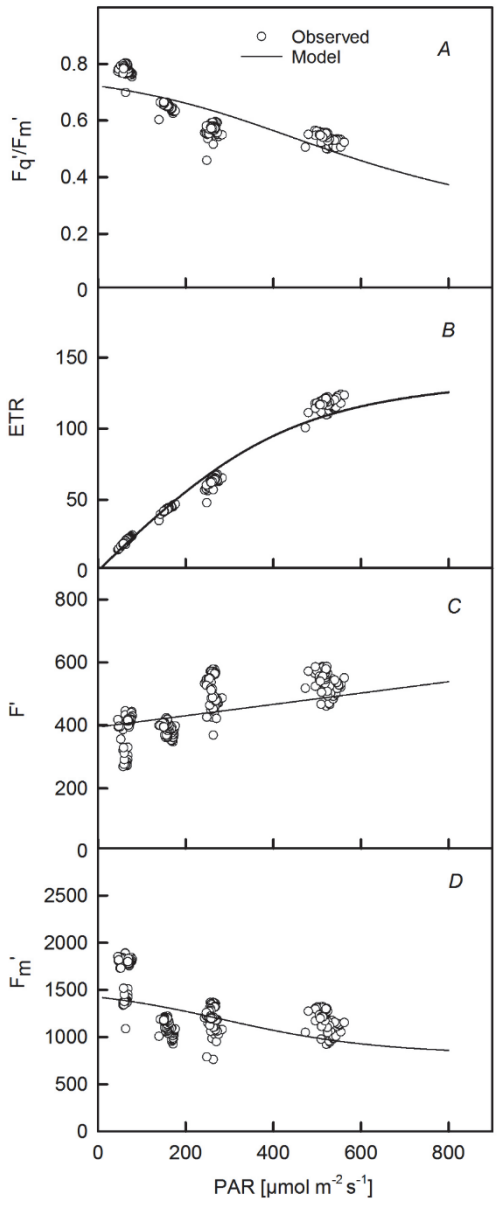

Fig. 2. The measured and predicted PSII-operating efficiency (*A*), electron transport rate (ETR) (*B*), fluorescence emission from leaf adapted to actinic light (F') (*C*), and maximal fluorescence (F_m') (*D*) as a function of light. Lines represent the model prediction and symbols are observation data. Growing temperature was 24°C and CO_2 concentration was 600 μmol mol^{-1}. The fluorescence was measured continuously every 30 min.

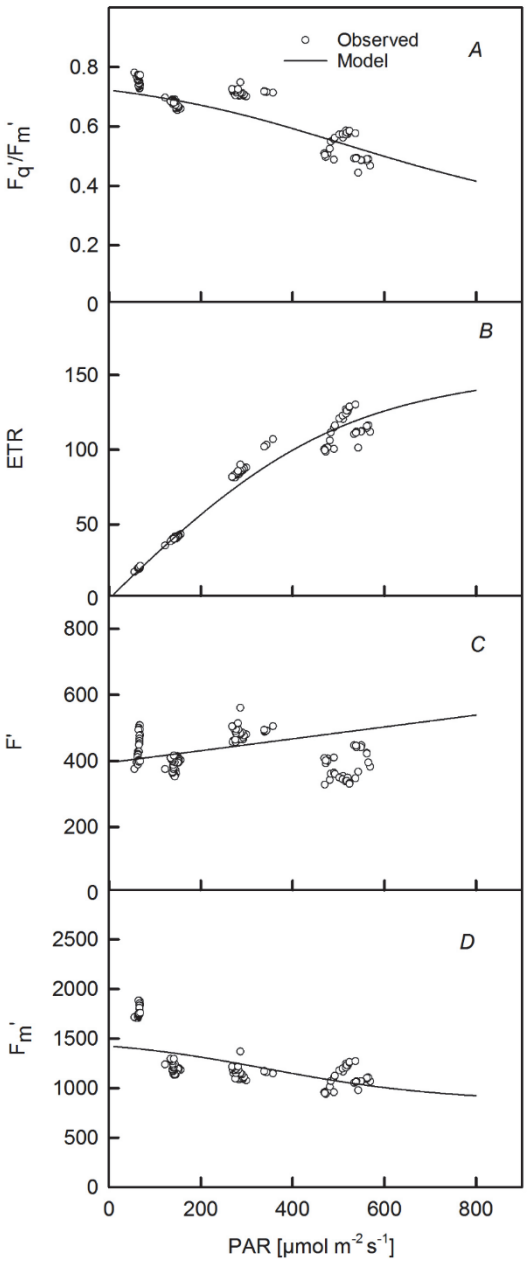

Fig. 3. The measured and predicted PSII-operating efficiency (*A*), electron transport rate (ETR) (*B*), fluorescence emission from a leaf adapted to actinic light (F') (*C*), and maximal fluorescence (F_m') (*D*) as a function of light. Growing temperature was 28°C and CO_2 concentration was 600 μmol mol^{-1}. Lines represent the model prediction and symbols are observation data. The fluorescence was measured continuously every 30 min.

and notably affected F' and F_m' values (Fig. 1). Consequently, the relationship between irradiance and F' and F_m' was weak compared with the growth chamber.

The model predicted F_q'/F_m' relatively well at 24°C (Fig. 2*A*), and 28°C (Fig. 3*A*), however, overestimation of F' or underestimation of F_m' affected prediction of F_q'/F_m'. An inverse relationship with F' and F_m', in addition to a low R^2 value for the relationship with irradiance (Fig. 1), might also affect an accurate prediction of the individual parameters, and F_q'/F_m'. Evans (2009) suggested F' was a function of irradiance, however, we used a positive linear relationship derived from F' and irradiance from measured empirical data to calculate F' and F_m'. Model performance was evaluated by comparing observed with predicted data. Rather than using the coefficient of determination (R^2), we assessed the performance of the model using RMSE and

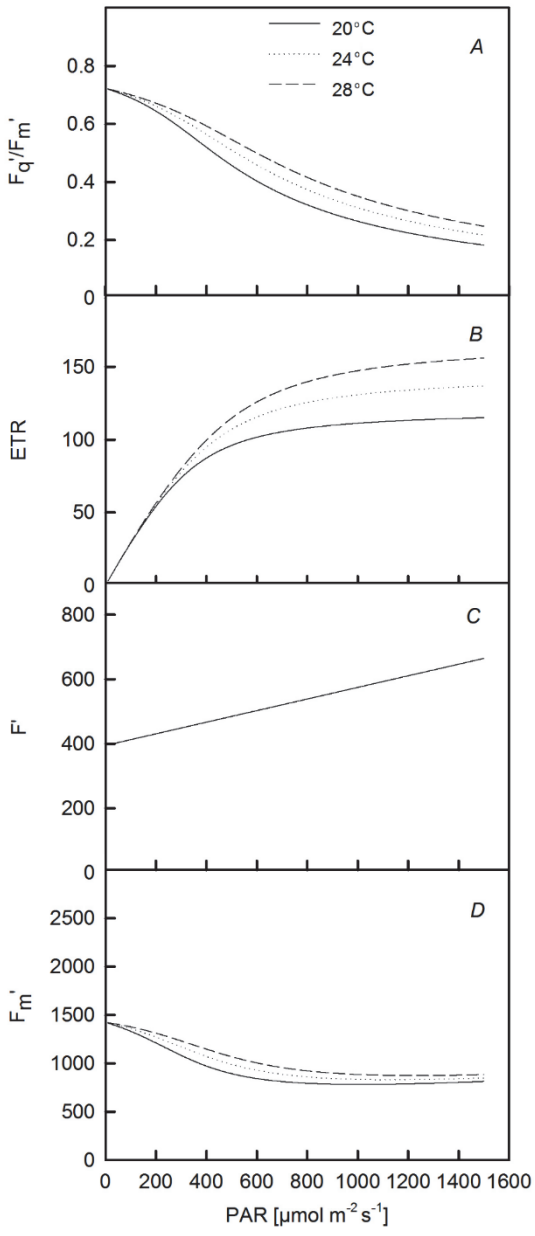

Fig. 4. Simulated PSII-operating efficiency (*A*), electron transport rate (ETR) (*B*), fluorescence emission from leaf adapted to actinic light (F') (*C*), and maximal fluorescence (F_m') (*D*) as a function of light at three different temperatures.

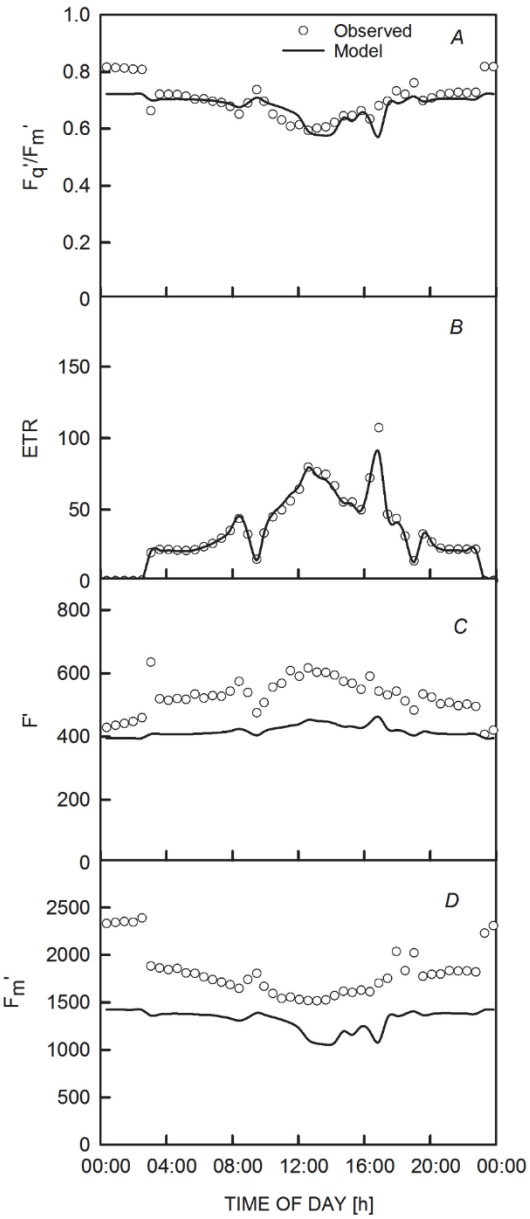

Fig. 5. Simulated PSII-operating efficiency (*A*), electron transport rate (ETR) (*B*), fluorescence emission from a leaf adapted to actinic light (F') (*C*), and maximal fluorescence from a leaf adapted to light (F_m') (*D*) on the day three of the observations. The irradiance and temperature were 30 min input values in the simulation. The growth temperature was 20°C in the growth chamber and 22°C (± 1.31) in the greenhouse, CO_2 was 600 μmol mol^{-1}. The fluorescence was measured continuously every 30 min using a monitoring PAM.

MSE. As previous studies have shown (Willmott 1982, Retta *et al*. 1991), R^2 and significance tests in general are often inappropriate or misleading when applied to compare model predicted and observed variables. RMSE and MSE indicated the model was weak in predicting F_m' with large RMSE and more negative MSE (Table 1). Similarly, F' comparisons between observed and modelled results were not adequate, with large RMSE and negative MSE, particularly at 32 and 36°C.

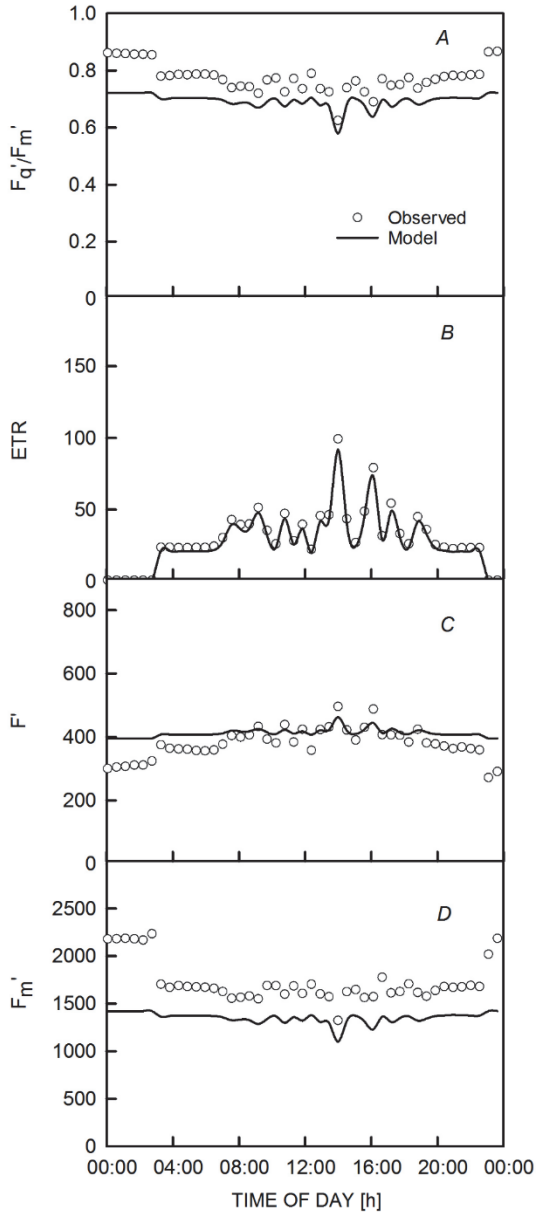

Fig. 6. Simulated PSII-operating efficiency (*A*), electron transport rate (ETR) (*B*), fluorescence emission from a leaf adapted to actinic light (F') (*C*), and maximal fluorescence (F_m') from a leaf adapted to light (*D*) on day six of the observations. The irradiance and temperature were 30 min input values in the simulation. The CO_2 and humidity was 600 µmol mol^{-1} and 60%, respectively. The fluorescence was measured continuously every 30 min using a monitoring PAM.

However, provided the F' and F_m' predictions were not robust, the model predicted F_q'/F_m' and ETR reasonably well. RMSE and MSE for observed and predicted values showed F_q'/F_m' and ETR were predicted reasonably well for all temperatures with the exception of 32°C (Table 1). Moreover, the F_q'/F_m' simulation under different temperature regimes showed a sharp decline with increased irradiance, which was directly associated with ETR under different temperatures (Fig. 4*A,B*). Genty *et al*. (1989) reported ETR being a function of F_q'/F_m' and irradiance. In our simulation, F_m' exhibited a temperature response related to F_q'/F_m' and ETR. F_m' showed increased differences between temperatures within a light range of 300–800 µmol(photon) m^{-2} s^{-1}, and the difference between temperatures was minimised above 800 µmol(photon) m^{-2} s^{-1} (Fig. 4*D*). This might be explained by the ETR reaching an optimum, and stabilising above 800 µmol (photon) m^{-2} s^{-1} for nearly all temperatures.

The F_q'/F_m' diurnal course simulation exhibited more reliable predictions near midday (Fig. 5*A*). ETR is directly related to irradiance, and therefore showed enhanced simulations throughout the day (Genty *et al*. 1989). However, F' and F_m' model simulations were lower than observations in most cases. Based on our analysis, the model inaccuracy in predicting F' and F_m' might result from the weaker light relationship. However, in our model little variation in F' with increased light, but large differences in daytime observations were observed. Results detected a strong relationship between F_m' and light, therefore the simulation showed a more consistent trend between the observations and decreased light during midday (Fig. 5*D*). Evans (2009) reported the F_m' response to irradiance differed between species, as well as on the upper and lower leaf surfaces.

In conclusion, enhanced F' and F_m' approximation and prediction facilitated PSII-operating efficiency predictions under different microclimate conditions. The approximation was simple, but required accurate fluorescence parameter estimations, which considered all factors that affected the parameters, rather than applying a simple linear equation to estimate F'. However, results indicated the approximation of fluorescence parameters can be much improved by testing different plant species. In doing so, the prediction capacity of the model can be strengthened; and the model's simplicity enables it to be implemented with online microclimate measurement data to monitor chlorophyll fluorescence and photosynthesis under extreme microclimatic conditions.

References

Baker N.R., Rosenqvist E.: Applications of chlorophyll fluorescence can improve crop production strategies: An examination of future possibilities. – J. Exp. Bot. **55**: 1607-1621, 2004.

Baker N.R.: Chlorophyll fluorescence: a probe of photosynthesis *in vivo*. – Annu. Rev. Plant Biol. **59**: 89 -113, 2008.

Evans J.R.: Carbon fixation profiles do reflect light absorption profiles in leaves. – Aust. J. Plant Physiol. **22**: 865-873, 1995.

Evans J.R., Vogelmann T.C.: Profiles of ^{14}C fixation through spinach leaves in relation to light absorption and photosynthetic capacity. – Plant Cell Environ. **26**: 547-560, 2003.

Evans J.R.: Potential errors in electron transport rates calculated from chlorophyll fluorescence as revealed by a multilayer leaf model. – Plant. Cell. Physiol. **50**: 698-706, 2009.

Farquhar G. D., von Caemmerer S., Berry J. A. *et al*.: A biochemical model of photosynthetic CO_2 assimilation in leaves of C_3 species. – Planta **149**: 78-90, 1980.

Genty B., Briantais J.M., Baker N.R. *et al*.: The relationship between the quantum yield of photosynthetic electron transport and quenching of chlorophyll fluorescence. – Biochim. Biophys. Acta **990**: 87-92, 1989.

Gijzen H.: Short-term crop responses. – In: Bakker J.C., Bot G.P.A., Challa H., Van de Brakk N.J. (ed.): Greenhouse Climate Control and Integerated Approach. Pp. 16-44. Wageningen Press., Wageningen 1995.

Guo Y., Tan J.: Recent advances in the application of chlorophyll *a* fluorescence from photosystem II. – Photochem. Photobiol. **91**: 1-14, 20015.

Harbinson J., Genty B., Baker N.R. *et al*.: The relationship between CO_2 assimilation and electron transport in leaves. – Photosynth. Res. **25**: 213-224, 1990.

Janka E., Körner O., Rosenqvist E. *et al*.: High temperature stress monitoring and detection using chlorophyll a fluorescence and infrared thermography in chrysanthemum (*Dendranthema grandiflora*). – Plant. Physiol. Bioch. **67**: 87-94, 2013.

Janka E., Körner O., Rosenqvist E., *et al*.: Using the quantum yields of photosystem II and the rate of net photosynthesis to monitor high irradiance and temperature stress in chrysanthemum (*Dendranthema grandiflora*). – Plant. Physiol. Bioch. **90**: 14-22, 2015.

Maxwell K., Johnson G. N.: Chloropyll fluorescence – a practical guide. – J. Exp. Bot. **51**: 659-668, 2000.

Murchie E.H., Lawson T.: Chlorophyll fluorescence analysis: a guide to good practice and understanding some new applications. – J. Exp. Bot. **64**: 3983-3998, 2013.

Retta A., Vanderlip R. L., Higgins R. A. *et al*.: Suitability of corn growth model for incorporation of weed and insect stresses. – Agron. J. **83**: 757-765, 1991.

Van der Ploeg A., Heuvelink E.: The influence of temperature on growth and development of chrysanthemum cultivars: a review. – J. Hortic. Sci. Biotech. **81**: 174-182, 2006.

Vogelmann T.C., Han T.: Measurement of gradients of absorbed light in spinach leaves from chlorophyll fluorescence profiles. – Plant Cell Environ. **23**: 1303-1311, 2000.

Vogelmann T.C., Evans J.R.: Profiles of light absorption and chlorophyll within spinach leaves from chlorophyll fluorescence. – Plant Cell Environ. **25**: 1313-1323, 2002.

Willmott C.J.: Some comments on the evaluation of model performance. – Bull. Am. Meteorol. Soc. **63**: 1309-1313, 1982.

Yin X., Struik P. C.: C_3 and C_4 photosynthesis models: An overview from the perspective of crop modelling. – NJAS-Wagen. J. Life. Sc. **57**: 27-38, 2009.

Appendix. Variables and parameters used in the model.

Symbol	Description	Unit	Value
E_J	Activation energy maximum electron transport rate	[kJ mol^{-1}]	37
S	Constant I. for optimum curve temperature dependent maximum electron transport rate	[kJ mol^{-1} K^{-1}]	0.71
H	Constant II. For optimum curve temperature dependent maximum electron transport rate	[kJ mol^{-1}]	220
θ	Convexity factor for response of J to irradiance	---	0.85
R	Gas constant	[J mol^{-1} K^{-1}]	8.314
$J_{max,25}$	Maximum electron transport rate at 25°C	[μmol m^{-2} s^{-1}]	210
J	Electron transport of a leaf	[μmol m^{-2} s^{-1}]	
T_{25}	Temperature in Kelvin at 25°C	[K]	298.15
c	Slope	---	0.43
k	Constant	---	395
β	Proportion of light absorbed by PSII	---	0.5
α	Fraction of incident light absorbed by a leaf	---	0.84
a_1	Fraction light absorbed in layer one	---	1
F_q'/F_m'	PSII operating efficiency	---	
$F_q'/F_m'_{,1}$	PSII operating efficiency calculated	---	
I	Incident light	[μmol m^{-2} s^{-1}]	
F	Fluorescence emission from leaf adapted to actinic light	---	
F_m'	Maximal fluorescence from light-adapted leaf	---	